Contents lists available at ScienceDirect

Automation in Construction

journal homepage: www.elsevier.com/locate/autcon

Machine learning-based classification of quality grades for concrete vibration behaviour

Shuai Fan [a,*], Tao He [a], Weihao Li [a], Chuang Zeng [b], Peng Chen [c], Lufeng Chen [d], Jiangpeng Shu [e]

[a] College of Mechanical Electronical and Engineering, Chengdu University of Technology, Chengdu, 610059, PR China
[b] Sichuan Road & Bridge Group Co., Ltd., Chengdu, 610041, PR China
[c] College of Engineering, Shantou University, Shantou, 515063, PR China
[d] School of Automation Engineering, University of Electronic Science and Technology of China, Chengdu, 610054, PR China
[e] College of Civil Engineering and Architecture, Zhejiang University, Hangzhou, 310058, PR China

ARTICLE INFO

Keywords:
Concrete vibration
Quality control
Cluster analysis
Shallow learning
K-means

ABSTRACT

The vibration behaviour of the vibrating rods is one of the key factors for the quality of concrete vibration that is essential for the long-term safety of concrete structures. Although many vibration operation regulations have been widely applied, evaluating method for concrete vibration samples is relatively rare. To fill this gap, this paper proposes a concrete vibration data acquisition system and attempts to perform a quality analysis of samples employing machine learning that amalgamates various parameters. The experimental results demonstrate that the data collection system to identify the vibration state achieves an accuracy of 93.75% and an accuracy of 90.3% in classifying vibration quality levels. The proposed method can classify and evaluate concrete quality levels, which strongly supports the visualization of concrete vibration process and the implementation of autonomous robot vibration. In the future, improving the reliability of the system and enhancing the accuracy of algorithms will be the focused.

1. Introduction

Concrete vibration is a crucial factor in determining project quality. It affects the economic, environmental, and social impact of the project, as well as the safety, reliability, and durability of the structure. Concrete vibration has attracted the attention of a vast range of engineering and architectural practitioners. Insufficient concrete vibration time can lead to improper settling of the concrete, resulting in various issues. Honeycombing, resulting from gaps or voids between coarse aggregate particles [1], is a prevalent concern in concrete construction [2]. Subsidence cracking presents a risk if the concrete does not vibrate properly, as inadequate settling can lead to surface cracks. Excessive vibration of the concrete can lead to multiple issues with the end product. These issues include the separation of the constituents of the blend, leading to an irregular surface. Over-vibration can also cause sand streaks within the concrete, which not only weakens the structure but is also unsightly. Additionally, excessive vibration can cause the loss of entrapped air within the concrete, resulting in a weaker and more prone cracking material [3]. To prevent these problems, it is crucial to monitor the vibration process carefully when working with concrete to ensure that the final product is strong and consistent throughout. In addition to the information mentioned above, concrete vibration specifications and manuals not only outline minimum requirements for vibration behaviour but also provide guidance on ideal vibration characteristics. These guidelines may include details on the frequency, amplitude, duration, and timing of the vibrations' application. It is clear that a comprehensive understanding of concrete vibration specifications and manuals is essential to achieve the desired outcomes in any project that utilizes this technology [4].

However, in actual practice, the manuals do not play a key role. In construction practice, the quality of concrete is often determined by conducting destructive test [5] or detecting cracks and bugholes on concrete surfaces [6] on hardened concrete. However, these methods can only monitor concrete weathering because of its compactness after vibration rather than timely prevention of concrete incompactness, so this method is not suitable for application in large vibrating fields because it is highly time-consuming and expensive. Thus, a large number of researchers have investigated real-time digital vibration. The digitization of vibration behaviour is an important aspect of concrete quality assessment. The indices that affect concrete vibration can be categorized into two groups.

* Corresponding author.
E-mail addresses: fansuai12345@163.com (S. Fan), 1439240566@qq.com (T. He), lwh19970521@163.com (W. Li), 675201393@qq.com (C. Zeng), dr.pengchen@foxmail.com (P. Chen), lufeng.chen@uestc.edu.cn (L. Chen), jpeshu@zju.edu.cn (J. Shu).

https://doi.org/10.1016/j.autcon.2024.105694
Received 11 March 2024; Received in revised form 5 August 2024; Accepted 8 August 2024

(1) The first group includes the effective radius of action and the optimum vibration time, which are influenced by various factors such as the type of concrete material, frequency and amplitude of the vibrator, reinforcement, and formwork layout.
(2) The second group of indices includes the duration of the vibration, position of the vibration and posture of the poker vibrator, which are mainly determined by the vibration behaviour and are equally important in determining the overall quality of the vibration.

With knowledge of both types of indices, we can make a comprehensive assessment of the overall quality of the vibration [7,8]. However, as mentioned above, although the importance of vibration is known and specifications and manuals on the vibration process have been reported, construction personnel and managers often lack knowledge of methods and tools to supervise and evaluate vibration quality, resulting in vibration quality depending largely on the experience and subjective judgement of workers. This has led to a decline in productivity in the past few decades in the construction industry [9–13].

Fortunately, the advancement of Artificial Intelligence (AI) has enabled computers to mimic human thinking and behaviour, facilitating comprehension and problem-solving [14]. Machine learning algorithms can make decisions based on previous experience and generate the most precise solutions by collecting and analysing data. It is crucial to select the relevant features in the dataset adequately and in sufficient quantity for the machine learning algorithm to solve the problem effectively [15]. Introducing machine learning to engineering problems can have a significant positive impact. However, there is a paucity of research investigating the application of machine learning techniques in concrete vibration. The majority of studies have focused on the monitoring of individual concrete indicators using diverse methodologies, with the resulting hardware devices often exhibiting suboptimal engineering and long layout times. Consequently, it is of significant academic interest to explore the potential of machine learning in the context of concrete vibration. Moreover, to the best of our knowledge, there is no general evaluation method that use a large number of concrete vibration samples to understand the characteristics of concrete quality grades using machine learning. Therefore, in this paper, we introduce machine learning with a data collection system composition to solve the problem of concrete vibration quality level assessment.

Research ideas are derived from a hybrid neural network recognition model to process the data stream developed by Quan's team. They enabled the automatic derivation of metrics related to vibration effectiveness and the first staged description of the concrete vibration process. A model for assessing the quality level of concrete vibration is proposed in this paper, using a concrete vibration data acquisition system and machine learning algorithms [16]. However, there is a paucity of research investigating the utilization of the raw concrete vibration data collected to grade the quality of vibration. Furthermore, the construction of the monitoring hardware for the majority of the studies was intricate and time-consuming. It is evident that engineering projects are not particularly amenable to such monitoring equipment. Consequently, the creation of a more engineering-oriented monitoring system is imperative. Additionally, the advancement of smart construction necessitates the automation of building construction. The integration of machine learning algorithms that can learn from previous concrete vibration experiences and autonomously make vibration decisions to maintain a high vibration quality level is crucial.

In this paper, we utilize the collected data for sample extraction and classify the vibration quality of each insertion and withdrawal cycle, thereby helping management personnel carry out more accurate monitoring to obtain more accurate concrete strength estimates. To extract samples of concrete vibration, a data monitoring and collecting system is developed, based on an Inertial Measurement Unit (IMU) and a current sensor. The system utilizes the IMU to gather acceleration and angular velocity data, which are then employed to calculate the velocity of the vibrating rod. Meanwhile, the current sensor collects data pertaining to the current, which is then used to determine the vibrating rod's status. As a result of this innovative combination of sensor types, the system is characterized by its simplicity, low cost, and numerous advantages. Furthermore, the effects of different methods were compared on vibration samples to assess the quality levels of the concrete vibration. This study's contribution lies in the innovation of the collection system that utilizes both inertial measurement units and current sensors. This study presents an innovative method for assessing the status of a vibrating rod. The method is based on a current change and allows for objective evaluations. The research presented in this paper contributes to enhancing the ultimate quality of concrete structures, enhancing the safety and economy of construction, and fostering the progress of intelligent construction.

The remainder of this paper is organized as follows. Section 2 provides a summary of the pertinent literature. Section 3 presents a detailed explanation of the proposed framework and methodology. Section 4 verifies the feasibility of the proposed method. Section 5 discusses the improvements of the experiments and future work of this paper, as well as suggestions for future work. The last section draws the conclusions of this paper.

2. Literature review

To classify the quality level of concrete, it is crucial to possess a thorough knowledge of the parameters that arise during concrete vibration. Past studies have suggested multiple techniques for comprehending the impact of vibration quality by employing a variety of sensor data combinations. This section now assesses different methods for monitoring concrete vibration parameters and describes the application of shallow learning in construction.

2.1. Monitoring the vibration quality of concrete

Only when the concrete is vibrated properly can the quality of the concrete be guaranteed. Although concrete vibration is an outstanding factor in concrete structures, there will still be some problems in the process of construction. Currently, because the process of concrete vibration is invisible, the quality of concrete vibration is decided by the subjective judgement of construction crews, which greatly limits the improvement of concrete quality. Many peer fellow researchers have endeavoured to address the issue of concrete vibration quality.

Common classifications of vibration quality ratings mainly include over-vibration, normal, and under-vibration [17]. It is important to note that, as stated in the research paper, missing vibration refers to the absence of vibration and is not considered in the classification of vibration grades. However, the avoidance of missing vibration is a prerequisite for the generation of vibration quality grades. As such, it is necessary to review the literature on missing vibration to enable a thorough analysis of quality classes of concrete. Specifically, this paper focuses on the classification of the quality of concrete vibration.

Chan et al. [18] investigated the impacts of normal and insufficient vibration on the consolidation and bonding of reinforcements for normal-slump concrete, High-Performance Concrete (HPC), and Self-Compact Concrete (SCC). These findings indicate that for the development of bond reinforcement in normal concrete, adequate vibration is indispensable, whereas HPC requires limited vibration. Olsen [19] employed accelerometers to gauge the pace of motion of a new concrete blend and determined the least amount of energy necessary to attain at least 97% consolidation. Due to the intricate nature of compacting concrete, particularly concerning multiple critical factors such as the vibrating frequency, amplitude, duration, and rheological properties of the mixture, few studies have explored the effects of vibration parameters on vibration quality.

Petrou et al. [20] utilized nuclear medicine techniques to examine the mechanism of concrete behaviour. The use of scintillation cameras

enabled the observation of the position of the vibrating rod in addition to depth information, facilitating the identification of any vibration leakage. The findings of this study provide significant insights into the fundamental characteristics of concrete.

Tian et al. [21] employed a dual-satellite system-based (Global Positioning System (GPS) and Global Navigation Satellite System (GLONASS)) tracking method to evaluate defects such as missing vibration, under-vibration, and over-vibration in the concrete placement process in a quantitative manner. The tracking system provides precise and timely remedial measures. This method enables the collection of vibration trajectory coordinates to mitigate missed vibration issues while simultaneously monitoring vibration status and duration.

Contrary to the low accuracy of indoor GPS, Gong et al. [22] highlighted the concrete quality issue due to insufficient real-time feedback of vibration data. They presented a Ultra-Wideband (UWB) positioning system to capture not only the position but also the duration of vibration. As a result, this system is suitable for both indoor and outdoor settings with high accuracy.

Tian et al. [23] presented a worldwide satellite navigation system aimed at tracing the vibration trajectory as a response to the issue of concrete consolidation under-vibration. This system is capable of determining the vibration status, calculating the vibration time, and promptly reporting any defects that appear, thus enabling timely remedial action.

Lee et al. [24] proposed a system framework that used computer vision and ultrasonic positioning to collect concrete vibration data. Moreover, based on this framework, Lee et al. [25] used ultrasonic sensors and electromagnetic sensors to collect vibration data, such as vibration duration and vibration state, from the vibration rod. This method can ensure real-time quality detection of concrete work. However, the proposed coordinate transformation calculation based on two ultrasonic sensors and three electromagnetic sensors for tracking and positioning seemed to be slightly cumbersome.

Many researchers jointly promoted that there is no specific assessment model to symbolize the relationship between the vibration effort and the quality of consolidation. For this question, Li et al. [26] proposed a model of vibration energy transfer in which the concrete vibration energy distribution is quantitatively characterized, and a visualization system was developed. Subsequently, the method was employed to assess the quality of vibration in reinforced concrete, thereby enabling workers to address substandard vibration areas in a timely manner [27].

The aforementioned study employs a number of traditional techniques with the objective of measuring the impact of vibration parameters on vibration quality for the purposes of quality control and enhancement. The rapid development of AI has led to the introduction of an increasing number of machine learning algorithms into the field of concrete quality monitoring.

Zhong et al. [28] employed a range of indicators, including the water-cement ratio, slump, insertion depth and vibration time, to assess the quality of concrete vibration. To gain a dynamic understanding of this quality, they employed the Random Forest algorithm.

Liu et al. [29] proposed positioning a concrete vibrating rod based on stereo vision, utilizing a stereo matching algorithm combined with a motion tracking algorithm to measure the vibration position and vibration depth. However, the shortcomings of machine vision are obvious, the sensitivity to light is very large, and whether to adapt to various lighting conditions still needs to be verified. Moreover, at present, real-time positioning of the rod utilizing machine vision is lacking, and this method is a platform for future research [30].

Wang et al. [31] contend that vibration quality depends critically on the duration and depth of vibration. Given the nonuniformity of concrete, they developed a concrete surface image classification model based on the ResNet-50 model to ascertain the optimal vibration duration and depth of vibration and to provide early warning of the vibration process. Building on this, in 2023, they introduced a visual method based on semi-supervised learning (Co-MixMatch) and data augmentation (StyleGAN2) to analyse the quality of concrete vibration by training a model [32]. This approach contributed to the field in a close way, as it enabled the development of a model that could be used to assess the quality of concrete vibration. Beforehand, Wei et al. [33] proposed a deep learning instance-level recognition and quantification method, which implements bugholes high-precision training tests on raw images of concrete surfaces. This approach aims to achieve improved quality and smoothness of concrete surfaces. Sun et al. [6] have proposed a method based on deep learning for the automatic detection of cracks and holes on concrete surfaces.

Quan et al. [17] introduced a technique for monitoring the position of a vibrating rod tip via a UWB sensor and an inclinometer. The Hopfield Neural Network (HNN) identification model they proposed can recognize the status of the vibrating rod. Nevertheless, the size of the inclinometer is significant, causing installations on the vibrating rod to be inconvenient, hampering the practicality of the technique.

Li et al. [34] determined the current difference threshold based on Simulated Annealing and Genetic Algorithms (SAGA) to determine the different working states of the vibrating rod (insertion, withdrawal, touching the reinforcement), through which the vibration time can be effectively detected to control the quality of concrete vibration.

Liu et al. [35] employed Convolutional Neural Networks (CNN) and image analysis techniques to accurately identify vibration times, thereby facilitating a rapid assessment of concrete vibration quality.

Ma et al. [36] proposed a method combining a Self-Attentive Feature Fusion Mechanism and a Multi-Scale Convolutional Neural Network (SE-MCNN) to identify and classify the vibration signals of concrete vibrators with high accuracy. This enables the accurate and quantitative assessment of the quality of concrete vibration.

Summarizing previous studies, Table 1 provides a clear picture of the indicators that previous researchers have focused on as well as the problems they have addressed.

This indicates that the utilization of machine learning methodologies to address concrete vibration issues is a favoured approach among a diverse range of researchers. However, in previous research, several scholars have suggested monitoring techniques for identifying faults in concrete vibration, including missing vibration, under-vibration, and over-vibration, which have yielded positive outcomes. However, the majority of these studies rely on a single vibration parameter (vibration time, depth and energy), with no clear categorization of vibration quality level. Consequently, under-vibration and over-vibration are typically evaluated based on vibration time alone, which lacks precision. Thus, this paper builds upon previous research in this field by employing a machine learning algorithm classification model to categorize concrete vibration samples into different quality levels.

2.2. Shallow learning in construction

Shallow learning comprises supervised learning [37], unsupervised learning [38], and reinforcement learning [39]. Unsupervised learning extracts knowledge from unlabelled data and focuses on data approximation and clustering issues. In contrast, supervised learning learns from labelled data to discover patterns and predict the outcomes of new inputs based on that pattern. Reinforcement learning [40] is a learning mechanism that maximizes the rewards obtained through learning.

Birnie et al. [41] utilized a decision tree algorithm to forecast the expenses of a home renovation contract. McCabe et al. [42] and their colleagues utilized Bayesian networks for assessing building performance. Baum et al. [43] used the Hidden Markov Model (HMM) algorithm for the probabilistic prediction of tunnel geology. Shu et al. [44] employed Support Vector Machine (SVM) to implement real-time monitoring of construction sites in construction projects. Furthermore, in 2017, Seong et al. [45] suggested a method to detect workers based on the colour pixels of their safety vests. The feasibility of human motion recognition

Table 1
Conclusion of previous researches.

Key technology	Year	Norm	Problems solved
Nuclear medicine technology	2000	Position	Behavioural mechanisms
GPS-RTK & GPRS	2013	Position	Missing vibration
UWB	2015	Position	Missing vibration
[a]Stereoscopic vision	2018	Position, depth, time	Missing vibration
[a]Random Forest	2018	Water-cement ratio, slump, depth, time	Quality assessment
GNSS & GPRS	2019	Status, time	Vibration defects
[a]Mask R-CNN	2019	Surface image	Bugholes identification
[a]Computer vision and ultrasonic positioning	2019	Status, time	Real-time monitoring
[a]Deep learning	2021	Surface image	Bugholes identification
[a]CNN & Internet of things	2021	Time, depth	Vibration defects
Vibration energy transfer model	2022	Power	Vibration energy
[a]UWB + inclinometer +HNN	2022	Position, time	Quality assessment
[a]Current sensor + SAGA	2022	Status, time	Quality assessment
Vibration energy transfer model	2023	Power	Reinforced concrete assessment
[a]Co-MixMatch + StyleGAN2	2023	Surface image	Quality assessment
[a]CNN + Image analysis	2023	Time	Quality assessment
[a]SE-MCNN	2023	Vibration signals	Quality assessment

[a] Indicates that the research involves machine learning.

in the field was studied by Ryu et al. [46] in 2019 using a wrist-worn accelerometer activity tracker.

The literature indicates that shallow learning can significantly aid in automating and enhancing intelligence in construction projects. This paper explores different shallow learning algorithms employed for predicting and categorizing concrete vibration samples. The vibration data acquisition system must ensure simplicity, reliability, and excellent engineering applicability while ensuring that the hardness of vibrated concrete remains within acceptable engineering thresholds. In this study, we combined cost-effective MENS IMU with a current sensor to collect vibration data in a manner that is popular among researchers. To gather vibration samples, it is necessary to extract features from vibration history data. Since the sample data are structured and influenced by shallow learning techniques, they remain the preferred form of an algorithm for processing structured data. Therefore, this paper employs a shallow learning algorithm to categorize vibrations.

3. Methods

This paper proposes the measurement and calculation of concrete vibration characteristics utilizing an IMU and a current sensor. The method is illustrated in Fig. 1 and explained below.

(1) The raw data of conventional vibration behaviour are collected.
(2) Concrete feature samples are extracted from the raw data.
(3) The samples are classified via an algorithm.
(4) The quality grade was obtained, and feedback was given to the vibrating rod.

We focus on explaining the vibration behaviour is defined by the raw data obtained from one insertion point to the next insertion point following the four processes of insertion, vibration, withdrawal and moving. And the raw data will be transferred to the computer via Universal Asynchronous Receiver/Transmitter(UART) for the purpose of saving and generating samples with different R. The eigenvalues of the samples are obtained through statistical and mathematical calculations and samples are classified by means of an algorithm.

3.1. Vibration data acquisition

The concrete vibration data acquisition system consists of a vibrating rod, sensor units, and controller units. The IMU is mounted inside the vibrating rod and connected to the Micro-Controller Unit (MCU) through a cable with an RS485 unit. The current sensor is connected to the MCU through another RS485 unit. Additionally, the wireless communication module requires a RS485 unit to be connected to the MCU. To facilitate construction operations, the controller unit and current sensor are enclosed in an external container. The wireless module communicates wirelessly with the external Wi-Fi router, and the Wi-Fi router transmits the collected data to the computer in real time for display. Additionally, the resulting data are saved to a storage device for near-term data processing. By setting up the logic, the data can display the status of the vibrating rod in real time. Samples were manually extracted from the raw data at various vibration stages and classified using machine learning techniques. Furthermore, the raw data of the entire vibration work are collected from the actual site.

Table 2
IMU parameter.

Parameter	Value		
Battery	3.7 V–260 mAh		
Size	36 mm*51.3 mm*15 mm		
Parameter	Acceleration	Angular velocity	Angular
Triaxial Ranging	±16 g	±2000°/s	X,Z ± 180° Y ± 90°
Stability	0.01 g	0.05°/s	–
Attitude accuracy	Dynamic 0.1°	Static 0.05°	–
Working frequency	TCP 1~10 HZ	UDP 1~200 HZ	–
Output	Time	Acceleration	Angular velocity

The technical specifications of the IMU are described in Table 2. The inertial measurement is used to measure triaxial acceleration and triaxial angular velocity. The current sensor can independently measure the work current of the vibrating rod. As shown in Fig. 2, the IMU measures 51.3 mm*36 mm*15 mm, is mounted in the vibrator rod with electrical adhesive tape and is connected to the external container through a cable, while the end of the cable is connected to the exterior container. A control unit, a current sensor, and a unit for wireless transmission are integrated within an exterior container. The external container contains a MCU and three RS485 modules, with the latter connecting to the MCU on one end and to the current sensor, IMU and wireless module on the other end, as shown in Fig. 3.

3.2. Vibration behaviour collection

This paper considers the energy absorbed by the concrete in a sample as the energy released by one vibrator insertion. The difference between the energy in the concrete at work and the idle energy is used to calculate the energy absorbed by the concrete at work. This is the reason why the current threshold is needed. The energy absorbed by the concrete was calculated using the following equation:

$$W = \int U I_{working} dt - \int U I_{threshold} dt \tag{1}$$

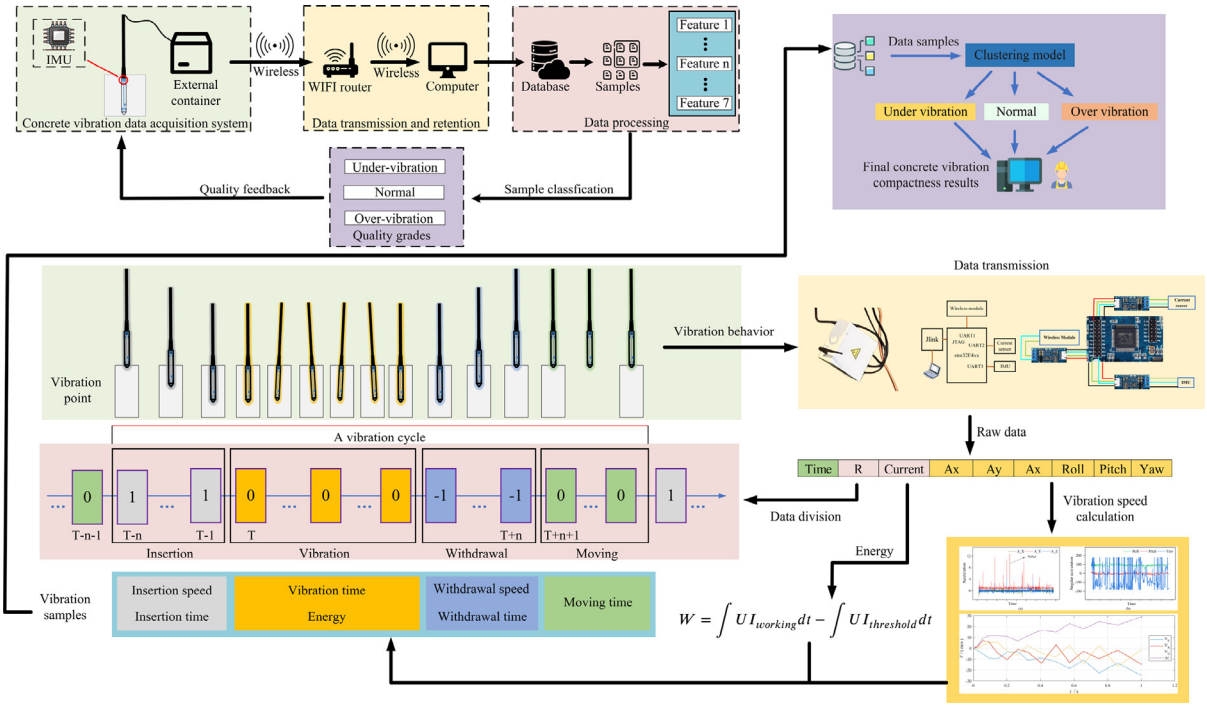

Fig. 1. Process for classifying the quality grades of concrete vibration.

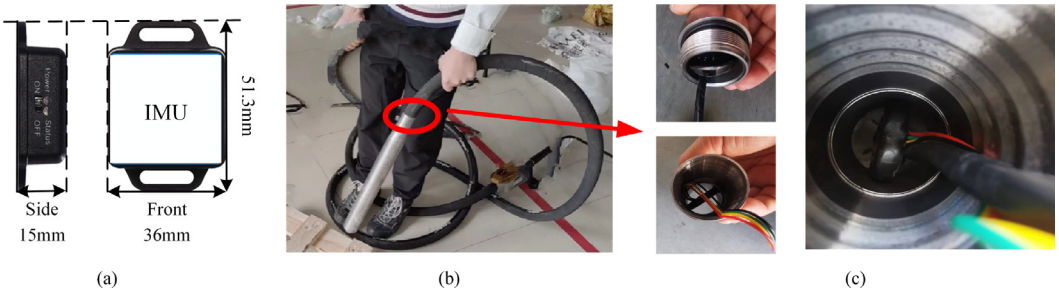

Fig. 2. Composition of vibrating rod: (a) IMU size; (b) IMU mounting position; (c) Position of the IMU inside the vibrating rod.

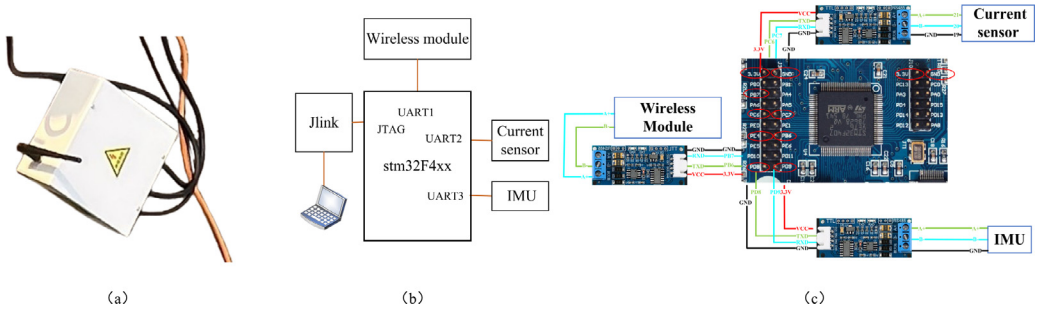

Fig. 3. Data transmission framework: (a) External container; (b) Communications infrastructure; (c) Chip unit connection.

where W denotes the energy absorbed by the concrete, U denotes the operating voltage (220 V), $I_{working}$ denotes the working current, and $I_{threshold}$ denotes the idle current of the vibrating rod.

Consequently, the features in Table 3 will be extracted.

3.2.1. *Data pattern and recognition feature for each stage of the vibration effort*

For concrete of the same type, there is a resemblance among dissimilar vibration quality levels resulting from the use of a uniform vibrating rod. This similarity can be employed to categorize the vibration quality

Table 3
Description of vibration features.

Feature	Time	Speed	Energy
Description	Insertion time Vibration time Withdrawal time Moving time	Insertion speed Withdrawal speed	Absorbed energy

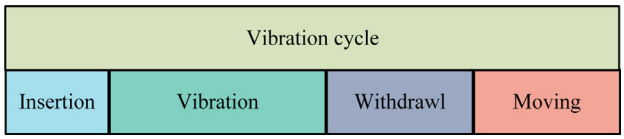

Fig. 4. Vibration cycle.

classes. Previous research has established three quality levels for vibrating rods: under-vibration, normal, and over-vibration. In this study, an unsupervised learning model was employed to cluster the obtained vibration samples into the three aforementioned categories.

The IMU collects the output of the gyroscopes and accelerometers, while the current sensor collects the information current when the vibrating rod works. The current measurement process requires setting the current threshold value. In this paper, the current when the vibrating rod is working in air is set as the required threshold. When the vibrating rod is inserted into the concrete, the current of the vibrating rod will be greater than the threshold, while the current of the vibrating rod stabilizes above and below the threshold when the vibrating rod is pulled out. The fluctuations above and below the threshold of the current are treated as the changes in the status of the vibrator. Therefore, the change in the current cycle can characterize the status of the vibrating rod. The value of the current above the threshold indicates that the status of the rod is insertion, while the value of the current below the threshold indicates that the status is withdrawal.

According to [17], the vibration process can be divided into four main processes: the insertion process, the vibration process, the withdrawal process and the movement process. As shown in Fig. 4, the insertion process, vibration process, withdrawal process and moving process are regarded as vibration cycles so that the whole vibration process consists of N vibration cycles.

In this paper, it is necessary to set the determined parameters At after measuring the current A of the working vibrating rod. The current threshold is set to a minimum of Max_value and a maximum of Max_value, to ensure the tightness of the logic. The relationship between the feature parameter At and the current threshold is shown in the equation.

$$At = \begin{cases} 3, At > Max\_value \\ 1, Mix\_value < At < Max\_value \\ 0. At < Mix\_value \end{cases} \tag{2}$$

The feature should be recorded to characterize the status of the vibrating rod. The characteristics of R are as follows:

$$R = At_{last} - At_{now} \tag{3}$$

The corresponding R value indicates the corresponding status of the vibrating rod. According to the size of the feature, the status of the vibration can be confirmed, and the relation is shown in Table 4. It is important to note that this paper employs a distinctive methodology for analysing the interaction between the vibrator bar and the reinforcement. When the vibrating rod makes prolonged contact with the reinforcement or becomes obstructed by it, the system provides feedback through the jamming detection algorithm, which is characterized by an eigenvalue R greater than 1. This is the period during which human intervention is required to address the issue. In the event that the mutual time is brief, the filtering algorithm will eliminate the transient. The Eq. (4) provides a brief summary of the aforementioned concept.

$$\mathrm{A_{mi}} = \left(\mathrm{A_i} + \mathrm{A_{i-1}} + \cdots + \mathrm{A_{i-Wmean+1}}\right) / \mathrm{Wmean} \tag{4}$$

where A_{mi} denotes the local mean filtering result, A_i represents the current of the vibrating rod and $Wmean$ is the size of the interval window.

Table 4
Relationship between R and the vibrating rod status.

R	The vibrating rod status
1	Insertion
0	Keep the status of the last
−1	Withdrawal
>1	Jamming

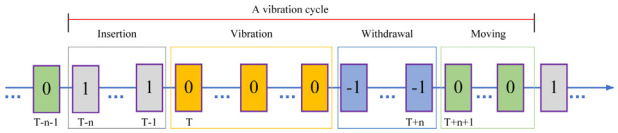

Fig. 5. State of the vibrating rod corresponding to the value of R.

In other words, all information about the state of the insertion vibrating rod can be obtained by the IMU and current sensors and then sent to the terminal computer by the Mono-Chip Computer (MCC) embedded in the Programmable Logic Controller (PLC). The data formats are shown in Table 5.

3.2.2. *Vibration speed calculation algorithm*

Although the error of the IMU diverges gradually with increasing in working time, the algorithms proposed in this paper can avoid the problem of the IMU. The logic of the system proposed in this paper is based on the feature value(R), which determines the working state of the vibrating rod. When the working state is switched, it is equivalent to a reset function. Accordingly, the IMU presented in Table 2 is deemed sufficient for the purposes of feature extraction.

Fig. 5 shows the variation in the R-value as a function of the change in the state of the vibrating rod and the time at which the initial state is set. When the state of the vibrating rod switches between two operating states, the rod velocity information at the moment of switching is set to the initial velocity of the IMU, which starts the recursion to the end of the next state change. In this way, the vibrating rod velocity information can be recursed through the state changes. Taking the inserted state as an example, when the rod is inserted, the moment when R changes from 0 to 1 serves as the initial state and starts recursion to the moment when the value of R changes from 1 to 0. In other words, each time the recursion process is executed, the error of the inertial sensor is reset to 0 once.

However, the IMUs also have certain errors, including quantization noise, angular random wander, angular rate random wander, zero-bias instability noise, and zero-bias repeatability. The details of the error analysis method can be found in Allan variance [47]. A specific discussion of the types of error is not elaborated here because that is not the focus of this paper. To solve the original data output from the IMU, the data first must be preprocessed as follows.

(1) First, the unit conversion and format transformation of the angular velocity and acceleration output from the IMU are needed.
(2) Second, the IMU velocity output used in this paper is in the form of a rate, and it is necessary to multiply the output acceleration by the interval time to obtain acceleration data in the form of an incremental acceleration to be used for inertial navigation system solving.

The coordinate systems used for the velocity solution are the world coordinate system (w system) and the carrier coordinate system (b system). The differential equation for the velocity update is:

$$\dot{\boldsymbol{v}} = \boldsymbol{R}_{wb}\boldsymbol{a} - \boldsymbol{g} \tag{5}$$

where $\boldsymbol{a} = [a_x \quad a_y \quad a_z]$ is the measured acceleration, R_{wb} represents the rotation matrix of b with respect to w and $\boldsymbol{g} = [0 \quad 0 \quad g_0]$ is the

Table 5
Format of collecting data.

Data	Time	R	Current	Acceleration	Angular velocity
Unit of data	Second (hh:mm:ss.000)	−1,0,1	A	g	°/s

gravitational acceleration. Then the generalized form of the velocity differential equation is:

$$\Delta \boldsymbol{v} = \left(\boldsymbol{R}_{wb}\boldsymbol{a} - \boldsymbol{g}\right)\Delta t \tag{6}$$

The corresponding median-based velocity update is expressed as follows:

$$\boldsymbol{v}_k = \boldsymbol{v}_{k-1} + \left(\frac{\boldsymbol{R}_{wb_k}\boldsymbol{a}_k + \boldsymbol{R}_{wb_k}\boldsymbol{a}_{k-1}}{2} - \boldsymbol{g}\right)(t_k - t_{k-1}) \tag{7}$$

3.3. Vibration behaviour prediction

For concrete of the same type, there is a resemblance among dissimilar vibration quality levels resulting from the use of a uniform vibrating rod. This similarity can be employed to categorize the vibration quality classes. For clustering in this particular application, a standard Euclidean K-means clustering algorithm was selected due to its ease of use and interpretability. The clustering performance of the K-means clustering algorithm is affected by several distinct features, including a significant dependence on initial conditions and clusters of different sizes, densities, and shapes [48,49]. Initially, the algorithm defines k centroids by selecting those that are the farthest from each other. Next, all remaining observations are assigned to the nearest centroid with the smallest Euclidean distance. Following the assignment of all observations to a group, k new centroids are calculated and the next iteration is conducted. The loop iteration continues until the centroids no longer change positions [50]. The optimal number of clusters was defined using the silhouette coefficient score, which ranges from −1 to +1. Higher values indicate greater cohesion among clusters, resulting in improved clustering. The contour coefficient is calculated by applying the following formula:

$$S(i) = \frac{b(i) - a(i)}{\max\{a(i), b(i)\}} \tag{8}$$

where, $a(i)$ represents the degree of cohesion among the sample points. The calculations are performed as follows:

$$a(i) = \frac{1}{n-1}\sum_{j \neq i}^{n} \text{distance}(i, j) \tag{9}$$

where j represents other sample points within the same class as sample i, and distance represents the distance between seek i and j. Therefore, the smaller $a(i)$ is, the closer the classes are, while $b(i)$ is calculated in the same way as $a(i)$.

For pragmatic purposes, the selection of the number of clusters relies on the desired number of clusters for structural analysis and is influenced by standards or the available computing power. Generally, it has been observed that selecting fewer clusters enhances cohesiveness among the clusters.

Previous research has established three quality levels for the vibrating rod: under-vibration, normal, and over-vibration. In this study, a K-means model was employed to cluster the obtained vibration samples into the three aforementioned categories.

4. Experiment and results

To extract samples and collect vibration experimental data, this paper established a concrete experimental data collection system in Section 3 and conducted data collection at the actual construction site. The collected data were then visualized and statistically analysed to prove that the system can effectively collect key parameters and identify the state of concrete vibration, thus aiding in quality control. The experimental data were used for sample extraction. The samples were then trained using both supervised and unsupervised learning methods. The accuracy of these methods is compared, highlighting the superiority of the K-means.

4.1. Experiment setup

The concrete vibration data acquisition system was set up at the construction site, as shown in Fig. 6. The IMU was integrated into the vibrating rod, while the vibration signal collector provided power and data transmission to the IMU via cables. Signals collected by the collector were then transmitted to the PC through Wi-Fi sensors. This study aimed to build on previous sensor installation techniques that involved fixing the sensor externally to the vibrating rod. However, in practical construction projects, the vibrating rod frequently contacts rebar. In certain areas, the presence of rebar hindered the complete insertion of the sensors, and, in some instances, caused them to be triggered, diminishing the usefulness of the project. Therefore, this paper describes the clever mounting of an IMU inside a vibrating rod in the context of a real project.

4.2. Data collection system validation and raw data collection of vibration samples

To ascertain the dependability of the methodology implemented in Section 3, it was necessary to test the compressive strength of the vibrated concrete. The chosen method involved utilizing rebound value measurements on vibrated concrete. Fig. 7 illustrates the arrangement of three boxes measuring 50 cm in length, 50 cm in width, and 60 cm in height. These boxes simulated three areas of vibration and were anchored by a wooden board and steel. Each box was labelled with a number from 1 to 3. The top of each box was designed with specific vibration points, which were targeted with a vibrating rod to initiate the vibration. The objective of the experiment is to test the efficacy of different regions, vibration behaviours, and our proposed recognition insertion and extraction algorithms, as well as interference algorithms. This will enable us to evaluate the correctness of our system and data algorithms, and to ensure the reliability of subsequent experiments. The experiment employed reinforced concrete with a design grade of C50 as the material type.

Experienced workers were employed to vibrate the concrete after pouring the three boxes, as shown in Fig. 8. The boxes were inserted diagonally and vertically, and the concrete vibration process was repeated twice for approximately ten seconds each time at the designated vibration points.

Fig. 9 indicates that there were no obvious defects on the surface or the sides of the concrete. The absence of defects on the surface of the concrete was not direct proof that the concrete did not have a compactness problem, which requires further testing. Rebound value testing of concrete can be a good representation of the strength of concrete. In accordance with the technical specifications for concrete compressive strength testing by the rebound method, 16 rebound values were obtained for the concrete to be tested. To calculate the average rebound value of the measurement area (Formula (10)), three maximum and three minimum values should be excluded.

$$R_m = \frac{\sum_{i=1}^{10} R_i}{10} \tag{10}$$

where R_m denotes the average rebound value of the survey area and R_i represents the ith rebound value.

Subsequently, the concrete strength($m_{f^c_{cu}}$) within the defined area of the structure can be calculated using the following formula:

$$m_{f^c_{cu}} = \frac{\sum_{i=1}^{n} f^c_{cu,i}}{n} \tag{11}$$

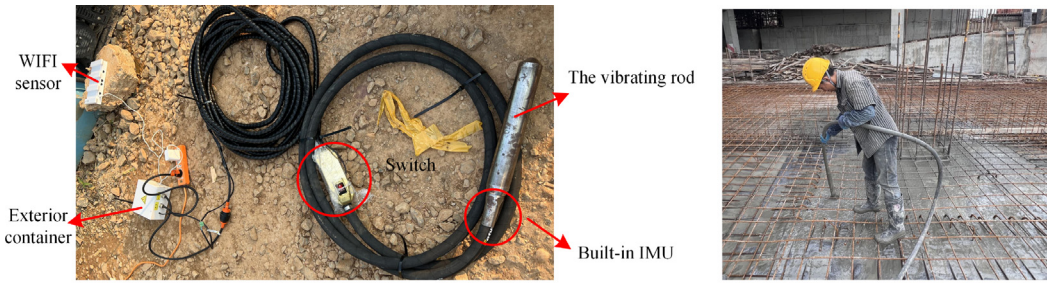

Fig. 6. Setup of the concrete vibration data acquisition system: (a) Vibrating rod; (b) Construction site.

Table 6
Concrete rebound value test.

Measurement point		1	2	3	4	5	6	7	8	9	10	11	12	13	14	15	16
Box	No.	Actual measurement of rebound value(R_m)															
Box 1	1	48	45	46	46	48	50	46	46	51	50	50	44	46	48	46	42
	2	46	44	48	49	47	47	48	46	42	46	41	43	42	47	50	50
	3	50	46	48	45	47	47	48	48	50	42	47	47	42	47	46	48
Box 2	4	45	41	46	39	45	47	48	41	46	48	45	44	44	46	50	44
	5	47	41	50	47	47	49	39	46	49	49	48	46	50	52	48	46
	6	44	44	33	47	43	46	47	47	46	49	38	50	47	35	47	48
Box 3	7	44	48	37	39	45	42	41	45	54	46	46	45	37	46	46	46
	8	42	40	42	44	46	47	47	41	42	49	49	42	47	43	47	46
Carbonation depth(d_m)		0.0	0.0	0.0	0.0	0.0	0.0	0.0	0.0	0.0	0.0	0.0	0.0	0.0	0.0	0.0	0.0

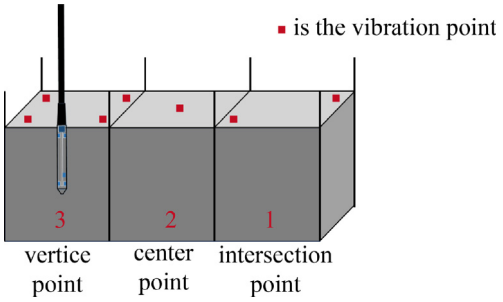

Fig. 7. Layout of the experiment.

where $f^c_{cu,i}$ denotes the concrete strength conversion values for the ith measurement area. f^c_{cu} is derived from the concrete strength conversion table for the survey area, utilizing the average rebound value R_m and the average carbonation depth value d_m, which are combined.

The rebound value test was performed on three vibrated boxes, and the results obtained are shown in Table 6. The average carbonation depth of the experimentally measured concrete was zero. The average rebound value and carbonation depth were used to calculate the concrete strength conversion values($f^c_{cu,i}$) for the test area, and the concrete strength was calculated using Formula (11). The results are shown in Table 7. It should be noted that the concrete strength($m_{f^c_{cu}}$) for the survey area points was obtained by excluding the three maximum and three minimum values of carbonation depth(d_m), according to the requirements of the rebound value calculation. The C50 reinforced concrete used in this paper accepts a rebound value of 44 or more. The results demonstrated that the vibrating rod system devised in this paper is capable of vibrating concrete to achieve satisfactory strength.

The validated vibrating rod system was utilized to collect real-time data from the concrete as it was being vibrated. The collected data were transmitted to the Wi-Fi sensor through the vibrating signal collector. Subsequently, the signal was displayed in real time on a PC and saved for future reference. To obtain relatively scientific and reasonable vibration samples, experienced vibration workers operated the vibrating rod and collected the vibration signals in this study.

The measurement duration was 1313.562 s, with a current threshold of 2.73 for the vibrating rod in the air. The inertial measurement unit was operated at a sampling frequency of 20 Hz. To ascertain the dependability of the value of R in Section 3.2.1, it is essential to compare the current data after binarization with the measured value of R. It is observed that the value of R signifies the state of the vibrating rod, while cyclical fluctuations of the current also demonstrate it. Nonetheless, the presence of R is necessary because it serves as a logistic variable, which aids in identifying the vibration period characteristics. Through embedded logic, the data collection system can receive real-time values for R. To enhance the effect of R, the current must be addressed through binarization. When the value surpasses the threshold, the outcome is assigned a value of 1. Otherwise, 0 is achieved. As demonstrated in Fig. 10, the binarization outcome of the current can be synced with the variation in R. By comparing the binarization outcomes of R and the current, the identification precision in Table 8 is 93.5%. Consequently, the value of R can determine the four vibrating rod statuses (insertion, vibration, withdrawal, and moving), as illustrated in Fig. 10(c).

For the velocity information of the vibration samples, the velocity solution formulas presented in Section 3.2.1 were used to determine the 3-axis angular velocity and 3-axis acceleration acquired by the IMU. The original experimental data from the IMU are plotted in Fig. 11. In this paper, the calculation of the instantaneous velocity of the insertion of the vibrating rod took the relative form. The purpose of such a calculation was to cleverly avoid the problem of error dispersion caused by the IMU solution. The specific calculation process is shown in Fig. 12. The average velocity is calculated as a characteristic of the vibration cycle recorded in the specimens.

The extracted feature data of the vibration cycle samples were summarized, and nine features were included, as shown in Table 9.

4.3. Comparison and selection of empirical models

To learn from the collected samples using supervised learning, it is necessary to calibrate the quality level of each concrete vibration sample. In this paper, experienced constructors are invited to calibrate the extracted vibration samples to ensure the accuracy of the sample target values.

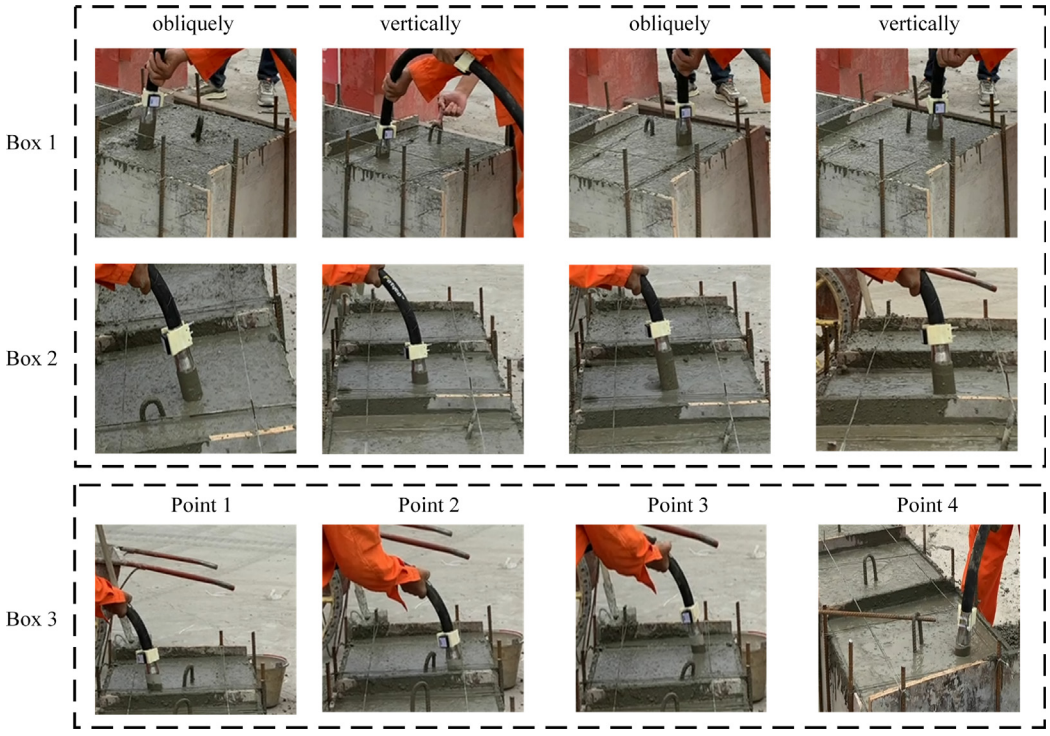

Fig. 8. Demonstration of actual verification operation.

Table 7
Calculation of concrete strength by rebound method.

10 rebound values		1	2	3	4	5	6	7	8	9	10	Strength ($m_{f^c_{cu}}$)	Average
Box	No.	Conversion value of concrete strength in the measurement area($f^c_{cu,i}$)											
Box 1	1	60.0	55.0	55.0	60.0	60.0	55.0	55.0	55.0	60.0	55.0	57	56.8
	2	55.0	50.4	60.0	57.5	57.5	60.0	55.0	55.0	48.1	57.5	55.6	
	3	55.0	60.0	57.5	57.5	60.0	60.0	57.5	57.5	57.5	55.0	57.8	
Box 2	4	52.7	55.0	52.7	57.5	55.0	52.7	50.4	50.4	55.0	50.4	53.2	55.8
	5	57.5	57.5	57.5	60.0	55.0	60.0	60.0	60.0	60.0	55.0	58.3	
	6	50.4	50.4	57.5	48.1	55.0	57.5	57.5	55.0	57.5	57.5	54.6	
Box 3	7	50.4	52.7	45.9	43.7	52.7	55.0	52.7	55.0	55.0	55.0	51.8	52.8
	8	45.9	45.9	50.4	55.0	57.5	45.9	57.5	48.1	57.5	55.0	51.9	

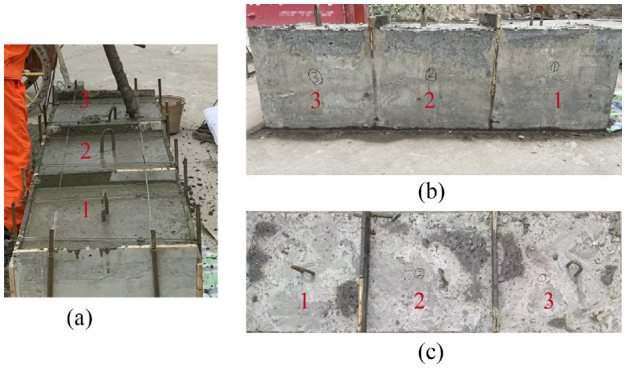

Fig. 9. Concrete surface after vibration: (a) Concrete vibration; (b) Side of the box; (c) Top of the box.

This paper employs several mature supervised learning algorithms, such as linear regression, K-Nearest Neighbour (KNN), logistic regression, decision tree, random forest, and SVM, to classify the concrete vibration samples into different levels. The accuracy of these algorithms are then compared.

Table 8
The recognition of accuracy.

	Vibration time (s)	Moving time (s)	Total time (s)
Measurement based on R	1033.353	280.208	1313.562
Value	1104.66	208.902	1313.562
Accuracy	93.5%		

Prior human classification calibration of the quality level of each vibration is required for supervised learning algorithms. To increase the credibility of the experiment, experienced workers were deliberately invited to calibrate the samples beforehand. The calibration is 0 for under-vibration, 1 for normal and 2 for over-vibration. The accuracy of various algorithmic classifiers on vibration samples was measured using the confusion matrix. The vertical axis of the matrix represents the actual sample labels, while the horizontal axis represents the predicted sample labels of the algorithmic classifiers. The diagonal of the matrix represents the accuracy of the classifier's prediction for that particular class. Fig. 13 demonstrates that all algorithms perform better under-vibration and over-vibration in all test results. The only difference lies in the evaluation of normal vibration.

Fig. 14 shows the scores of the classifiers calculated under different train sets. The decision tree outperforms the other four classifiers, while the linear regression is the least accurate.

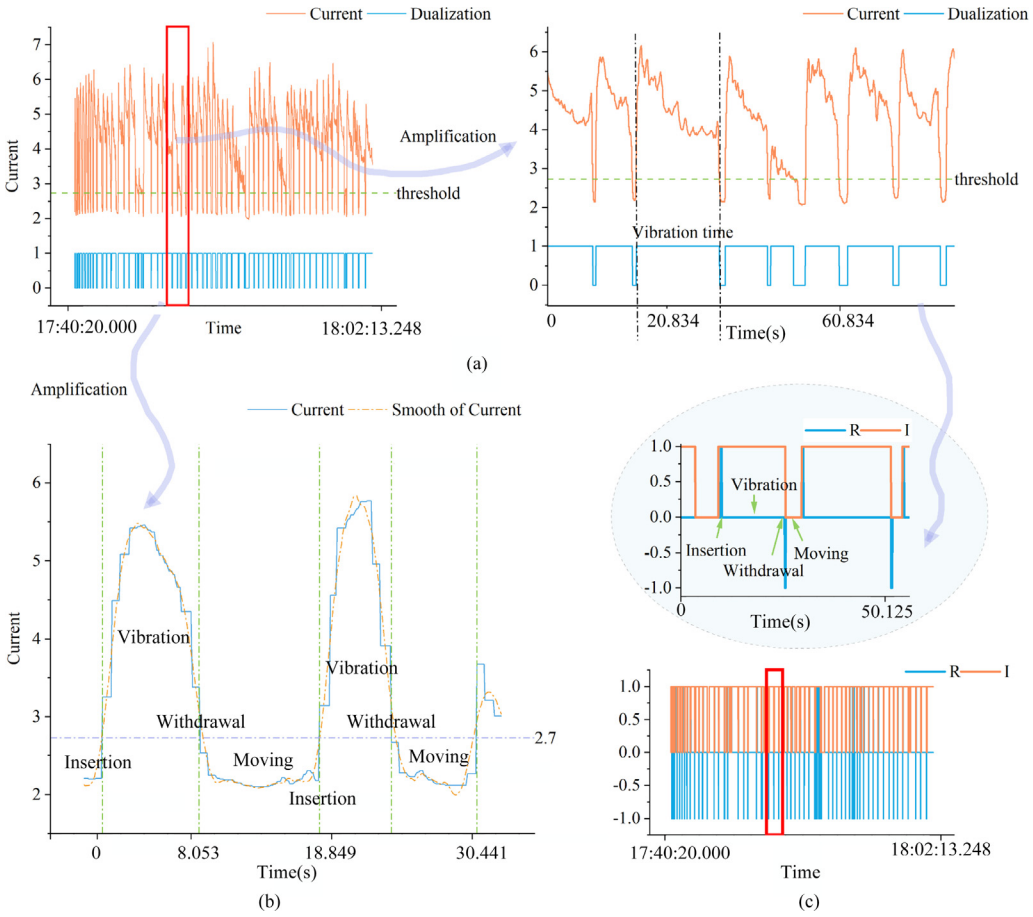

Fig. 10. Signal data processing: (a) Current binarization; (b) Status of current recognition; (c) Comparison of the current and R.

Table 9
Vibration cycle samples.

Sample	Insertion time	Vibration time	...	Insertion speed (y)	Insertion speed	...	Absorbed energy
1	0.248	2.949	...	3.335	5.418	...	1566.094
2	0.35	1.75	...	1.467	4.741	...	1212.545
3	0.248	0	...	4.724	5.91	...	116.939
			...			...	
			...			...	
29	0.252	21	...	4.179	5.106	...	11 152.733
30	0.253	12.845	...	1.84	3.91	...	7721.052
			...			...	
			...			...	
66	0.252	21.539	...	4.59	5.27	...	8620.401
67	0.25	25.741	...	3.813	4.884	...	6908.706

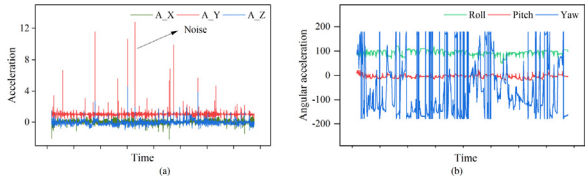

Fig. 11. Original data of IMU: (a) Acceleration curves; (b) Attitude angle curves.

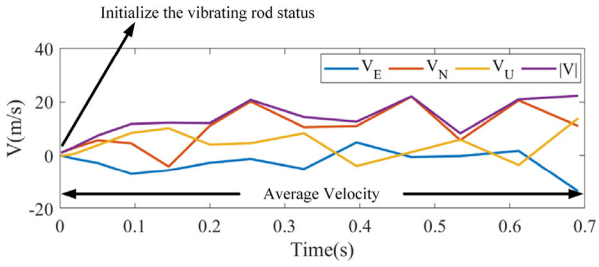

Fig. 12. Speed initialization and calculation of average speed.

To classify concrete vibration samples via unsupervised learning, calibration of the concrete vibration sample class is unnecessary. This paper employs nine common clustering algorithms (Table 10) to cluster the vibration samples.

As shown in Fig. 15, the clustering results of different algorithms based on features were visualized. The graph displays sample points,

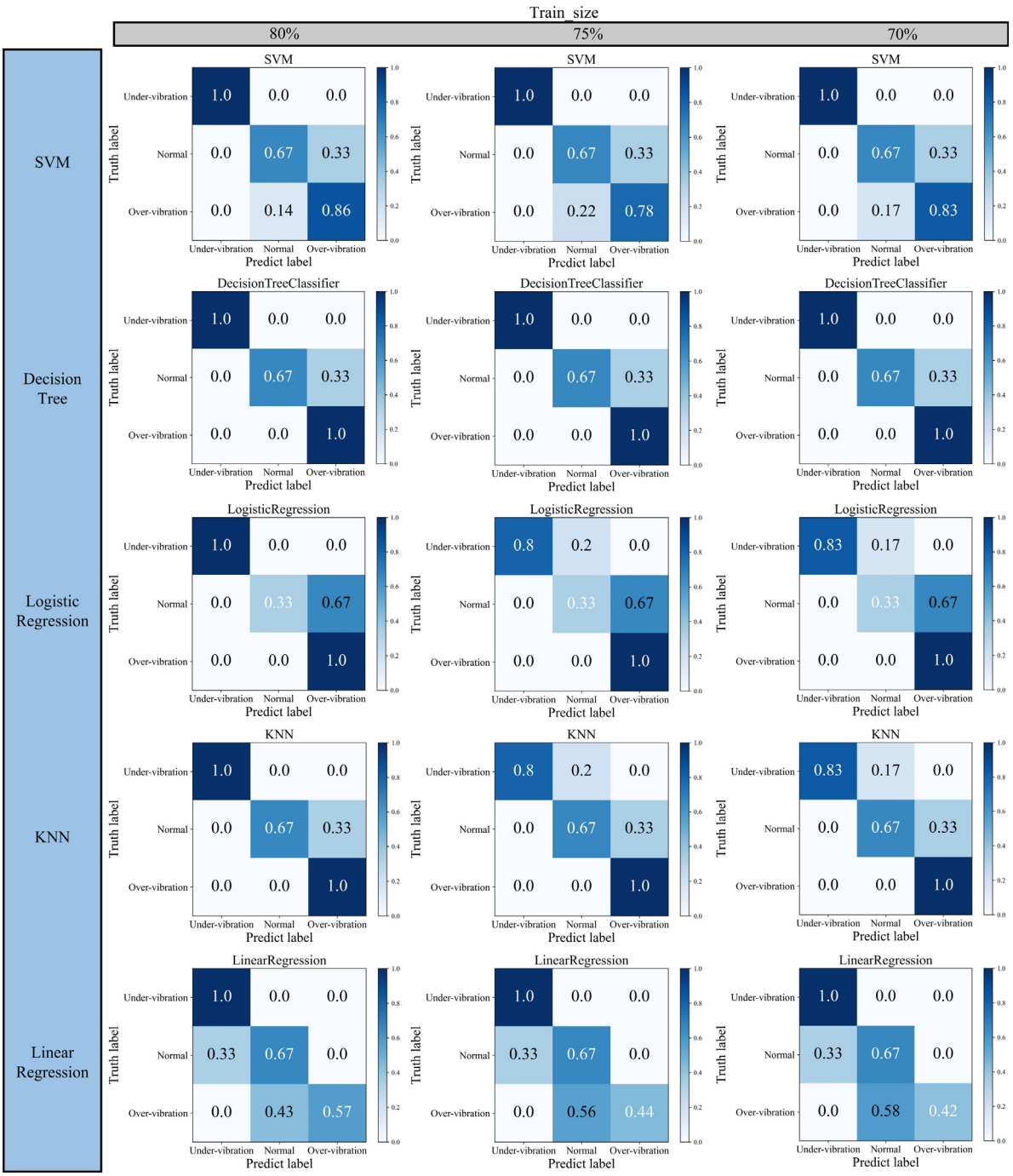

Fig. 13. Comparison of five supervised learning algorithms.

with different colours representing varying levels of vibration quality. Affinity propagation (AP, in Fig. 15(a)) and Density-Based Spatial Clustering of Applications with Noise (DBSCAN, in Fig. 15(d)) cannot achieve the expected classification effect, i.e. AP classifies all samples one by one, whereas DBSCAN classifies the datasets into a category. Therefore, the two algorithms cannot be used. Although the Mean Shift (in Fig. 15(g)) and the Ordering Points To Identify the Clustering Structure (OPTICS, in Fig. 15(h)) can achieve the goal of classification, the four categories obtained are not the result that we wanted for out method. Compared with the above four algorithms, Agglomerative Clustering, Balanced Iterative Reducing, and Clustering using Hierarchies (BIRCH), K-means, mini-batch K-means, and Gaussian Mixture Model can achieve to classify the samples into three categories. However, the silhouette coefficient (SC) and Calinski–Harabasz (CH) coefficient of each algorithm need to be calculated so that the strengths and weaknesses of the algorithm can be determined. The different SC indices and CH indices of the algorithms are shown in Table 11. In contrast, the K-means algorithm does a better job of classifying the samples into the desired three categories.

To increase the independence of the data features and to alleviate the problems caused by sample dimensionality, the data samples should undergo dimensionality reduction via principal component analysis and the K-means algorithm should be used to cluster the data again. Correlation analysis was carried out on the sample features, as shown in Fig. 16. Obviously, the correlation coefficient between the vibration time and the absorbed energy of concrete reaches 94%, while the correlation coefficient between the withdrawal speed (y) and the withdrawal speed is 69%. For the correlation analysis of data features, we can find

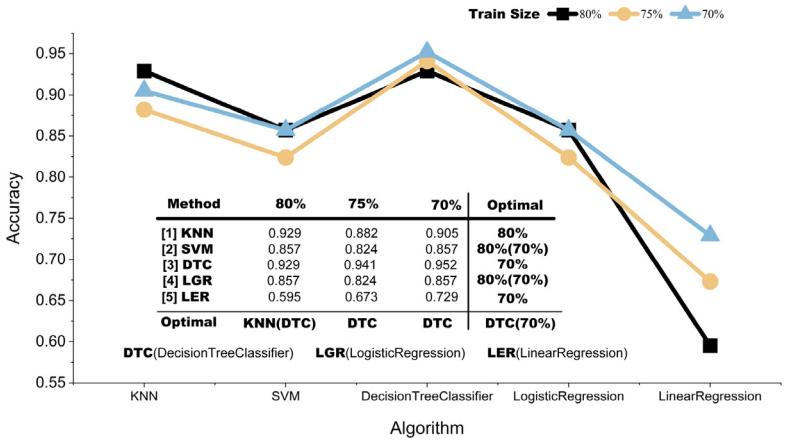

Method	80%	75%	70%	Optimal
[1] KNN	0.929	0.882	0.905	80%
[2] SVM	0.857	0.824	0.857	80%(70%)
[3] DTC	0.929	0.941	0.952	70%
[4] LGR	0.857	0.824	0.857	80%(70%)
[5] LER	0.595	0.673	0.729	70%
Optimal	KNN(DTC)	DTC	DTC	DTC(70%)

Fig. 14. Scores of the classifiers calculated under different train sets.

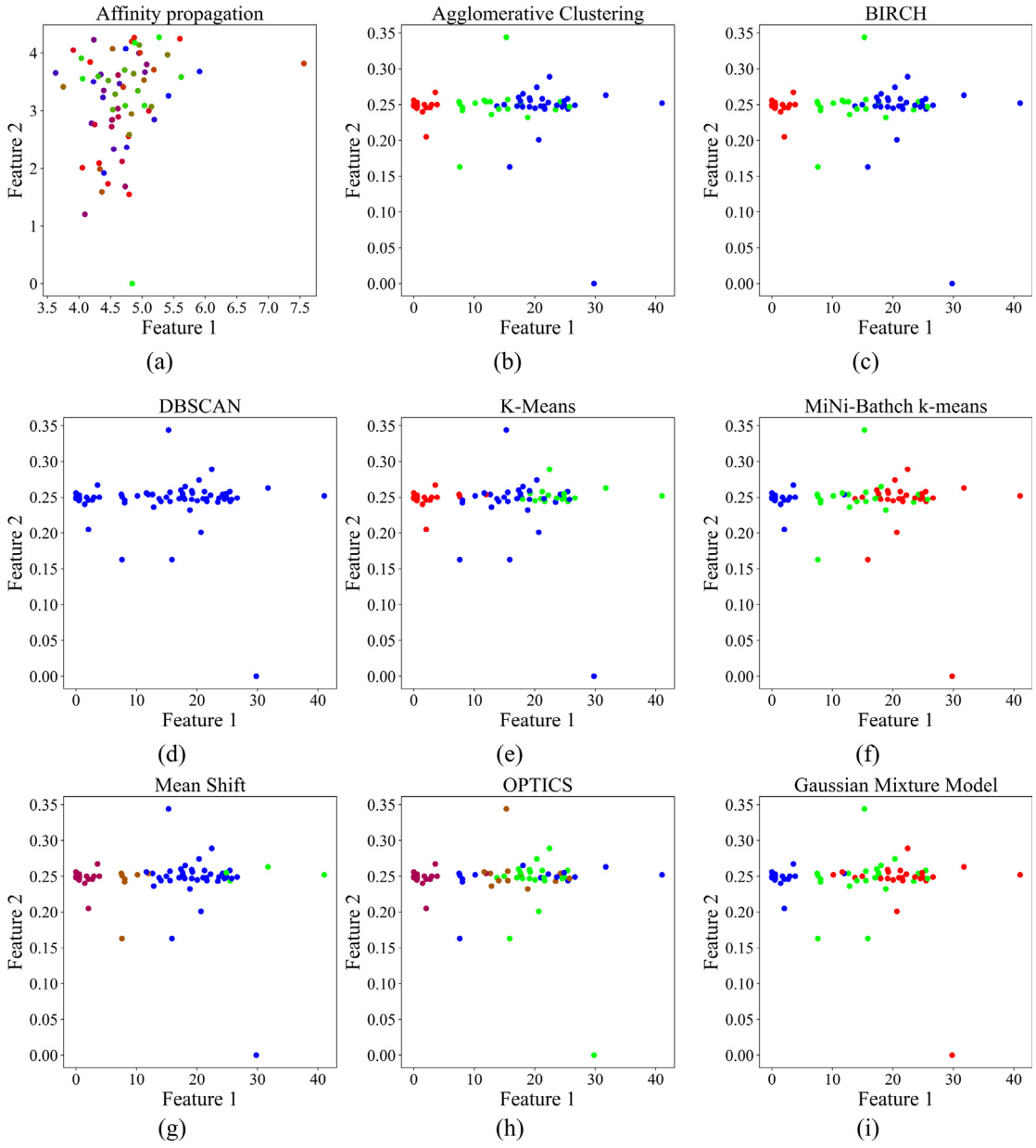

Fig. 15. Clustering effects of nine algorithms.

Table 10
Clustering algorithms.

Clustering algorithm	Description
Affinity propagation	A graph-theoretic clustering algorithm that derives the final clustering result by calculating the similarity between data points.
Agglomerative	A bottom-up clustering algorithm that treats each data point as an initial cluster and progressively merges them into larger clusters until a stopping condition is reached.
BIRCH	A clustering algorithm based on hierarchical clustering that can handle large-scale datasets quickly and works well for clusters of arbitrary shape.
DBSCAN	A density-based clustering algorithm that efficiently discovers arbitrarily shaped clusters and is able to handle noisy data.
K-Means	An algorithm that iteratively searches for optimal cluster centre locations until a state of convergence is reached.
MiNi-Batch k-means	An algorithm for optimized K-Means that uses a small subset of data to reduce computation time while still attempting to optimize the objective function.
Mean Shift	A density-based non-parametric clustering algorithm that identifies clusters in data by finding the location with the highest density of data points.
OPTICS	A density-based clustering algorithm that automatically determines the number of clusters and also finds clusters of arbitrary shapes and is able to handle noisy data.
Gaussian Mixture Model	A clustering algorithm based on probability distributions that assumes that each cluster conforms to a different Gaussian distribution (the data within each cluster will conform to a certain data distribution).

Table 11
Comparison of algorithmic strengths and weaknesses.

Algorithm	Silhouette coefficient	Calinski–Harabasz
Agglomerative silhouette	0.60311939	199.878559
Birch	0.60311939	199.878559
K-means	0.577387272	218.6854658
Mini-Batch-KMeans	0.601892569	210.9485397
Gaussian Mixture	0.398971454	132.2793682

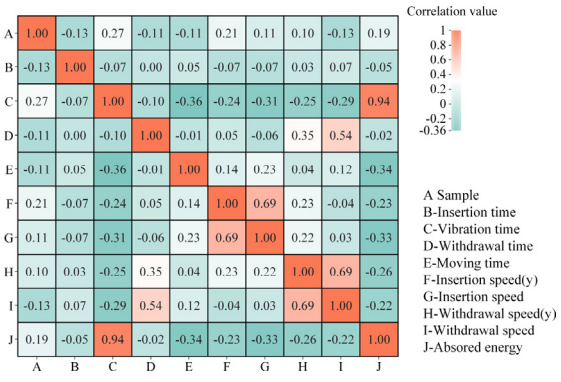

Fig. 16. Correlation analysis of vibration samples data.

redundant information in the original high-dimensional space as well as a noisy sound system, which will affect the accuracy, so the data can be reduced to achieve the extraction of effective information synthesis and useless information discarded.

In this paper, Principal Component Analysis (PCA) is used to transform a series of potentially linearly correlated variables of a sample into a new set of linearly uncorrelated variables, so that the new variables can be used to demonstrate the characteristics of the data in smaller dimensions. Fig. 17 shows the results of cluster analysis after PCA based on the K-means method. Clustering can achieve an excellent effect according to the characteristics of the vibration samples. The green parts indicate quality level of normal vibration, the red parts indicate under-vibration, and the yellow parts indicate over-vibration. The K-means treated with PCA performs better in terms of sample compactness than does the standalone K-means algorithm.

The sample data will be manually labelled with vibration grade using the combination of the mixing and solidification manual combined

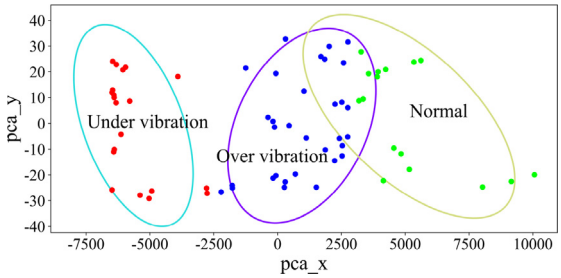

Fig. 17. K-Means clustering after PCA: (green) normal vibration; (red) under-vibration; (blue) over-vibration.

with the advice given by professional vibration workers to compare the clustering effect as shown in Table 12. The average accuracy reaches 0.903.

5. Discussion

This study is the first attempt to apply data sampling and machine learning methods to evaluate the internal concrete vibration quality. Compared to previous studies, the following innovations and modifications have been made.

(1) In terms of hardware, the concrete vibration data acquisition system innovatively integrates the IMU and the current sensor. The IMU has the characteristics of high integration, high accuracy in a short time, and strong robustness. The idea of this paper is to use the concept of relative speed to calculate the speed with an IMU. In addition, the cost of concrete vibration equipment will be reduced. In addition, IMUs are a futuristic technology with great potential.
(2) The process of vibration is divided into n cycles. Typical data features for each of the four stages in a cycle are extracted to form a sample concrete vibration cycle. These samples can be used as vibration experience on which machine learning algorithms can base their vibration quality decisions, achieving independence from manual evaluation.
(3) This study evaluated machine learning algorithms for classifying concrete vibration samples. It compares supervised and unsupervised learning under different test sets to identify the algorithm that best classifies vibration quality levels. This paper

Table 12
Comparison of clustering results with human calibration results.

Manual labels				Prediction labels		
Labels	Over vibration	Normal	Under vibration	Over vibration	Normal	Under vibration
Number	33	18	17	32	16	20
Accuracy				0.970	0.889	0.850
Average accuracy				0.903		

proposes a method for classifying concrete quality classes based on a rudimentary algorithmic model. One of the future research directions is to explore a better learning algorithm for vibration quality class classification criteria.

However, there are still some limitations that warrant further research. First, this study proposes a hardware prototype solution to calculate the velocity of a vibrating rod. Although the IMU result can be solved, the positioning accuracy is not validated in reality. Perhaps integrated navigation can improve positioning accuracy, but an interdisciplinary method may be required to solve this problem. Second, due to the limitations of the experimental conditions, it must be noted that the data sample size for this paper is only 68. As such, it is likely that this sample size is too small and may lead to overfitting of the data. It is important to collect a larger number of vibration cycle samples in future work to characterize and analyse the vibration quality level thoroughly as well as develop subsequent determination criteria. In addition, we specifically find that when employing the K-means clustering method to cluster vibration cycle samples, this study deliberately divided the samples into three categories. However, this study investigated the size of the silhouette coefficient for various numbers of clusters, as illustrated in Fig. 18. The K-means method yielded the lowest silhouette coefficient score when the vibratory quality effects were partitioned into the three typical categories. Upon closer examination of the samples, it was found that the presence of the two samples with zero vibration time may have contributed to the phenomenon of missing vibrations. Due to the presence of missing vibration, there were four categories in the samples, including under vibration, over vibration, normal, and 0 vibration time. This resulted in the highest silhouette coefficient at K = 4, which is also a realistic outcome. The next step is for the trained clustering model to be applied in actual vibration operations to provide real-time feedback of quality ratings to the construction crew, which is a significant area for future research. The process is demonstrated in Fig. 19. Using the vibration cycle extraction principle outlined in this paper, *N* vibratory cycle samples are generated by extracting the vibration behaviour. The clustering training model is employed to classify the quality level of the resulting vibration samples. Real-time visualization of the quality level of the vibration cycle enables construction personnel to monitor the vibration operation as it progresses. The fourth point pertains to the metric measuring leak vibrations, which is not covered in this study. Based on the sample data, the average movement time is approximately 4.12 s, while the dispersion time of the inertial sensor is approximately 2 s; however, these values fail to meet the positioning required level of accuracy. Therefore, future research should explore the use of more expensive sensors or incorporate combined navigation to enhance leak metrics.

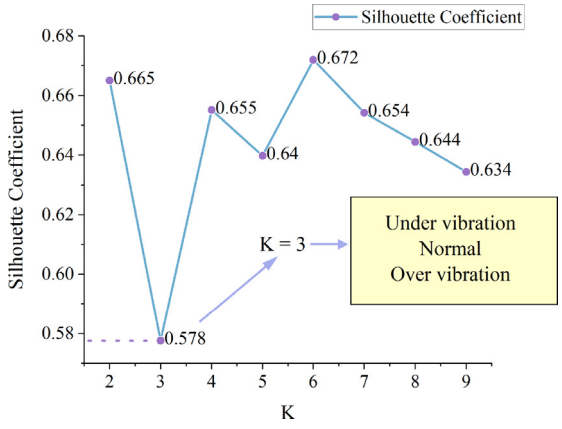

Fig. 18. Different K corresponding to silhouette coefficient.

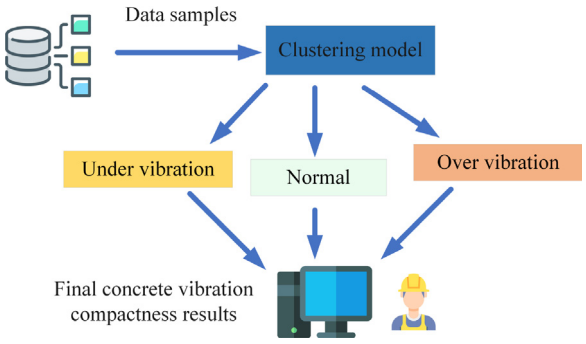

Fig. 19. Prediction model.

6. Conclusions

This paper presents a complete set of concrete vibration data collection methods with two aspects: an evaluation method and hardware. A general standard of machine learning is established to evaluate the final concrete vibration quality level.

(1) The hardware of the concrete vibration data collection method integrates the IMU and a current sensor. The actual application shows that this hardware combination has a simple composition, is reliable, expandable, and robust, and has a low cost. This significantly minimizes the time cost and financial outlay required for the construction of hardware in concrete vibration monitoring, thereby accelerating the overall project timeline.

(2) The experimental results demonstrate that the classification prediction accuracy reaches 90.3% in this paper compared with the traditional manual calibration results. The pioneering use of vibration behavioural feature samples to classify and predict vibration quality levels has the potential to promote the application of machine learning techniques to engineering and construction.

This paper represents a significant advance in the field of vibration monitoring, offering a novel approach to addressing the limitations of previous studies that have focused on the issue of missing vibrations in real time. The vibration samples captured in this study offer valuable engineering experience that can be retained and serve as a benchmark for future vibration operations. As the number of vibration samples increases in the future, this experience will become increasingly sophisticated, leading to enhanced vibration quality. Concurrently, the deployment of machine learning methodologies for the classification and assessment of vibration quality has also nearly mitigated the trend of declining talent in contemporary construction work.

Declaration of competing interest

During the preparation of this work, no generative AI is used. The authors declare that they have no conflict of interest, and this study was funded by the Natural Science Foundation of China (52005082, 52105111), Natural Science Foundation of Sichuan Province (2023NSFSC0866), the Basic and Applied Basic Research Foundation of Guangdong Province through Grant 2022A1515010859, the Guangdong Provincial Science and Technology Special Fund Project through Grant STKJ2021171, and the Shantou University (STU) Scientific Research Initiation Grant through Grant NTF21029.

Acknowledgements

The authors gratefully acknowledge the financial support that is provided by the Natural Science Foundation of China (52005082, 52105111), Sichuan Science and Technology Program (2023NSFSC0866), the Basic and Applied Basic Research Foundation of Guangdong Province through Grant 2022A1515010859, the Guangdong Provincial Science and Technology Special Fund Project through Grant STKJ2021171, and the Shantou University (STU) Scientific Research Initiation Grant through Grant NTF21029.

References

[1] S. Popovics, A review of the concrete consolidation by vibration, Matér. Constr. 6 (6) (1973) 453–463, http://dx.doi.org/10.1007/bf02473784.
[2] The Bughole problem, ACI J. Proc. 69 (3) (1972) http://dx.doi.org/10.14359/11260.
[3] 309 ACI Committee, Behavior of fresh concrete during vibration, ACI J. Proc. 78 (1) (1981) 36–53, http://dx.doi.org/10.14359/6909.
[4] Richard E Miller, Neil A Cumming, Timothy P Dolen, Chiara F Ferraris, Steven H Gebler, Glenn A Heimbruch, Kenneth C Hover, Garry R Mass, Bryant Mather, Larry D Olson, Jerome H Ford, H Celik Ozyildirim, Steven A Ragan, Mike Thompson, Bradley K Violetta, Guide for consolidation of concrete, ACI Mater. J. 84 (5) (1987) http://dx.doi.org/10.14359/1613.
[5] Xiaojian Gao, Junyi Zhang, Yue Su, Influence of vibration-induced segregation on mechanical property and chloride ion permeability of concrete with variable rheological performance, Constr. Build. Mater. 194 (2019) 32–41, http://dx.doi.org/10.1016/j.conbuildmat.2018.11.019.
[6] Yujia Sun, Yang Yang, Gang Yao, Fujia Wei, Mingpu Wong, Autonomous Crack and Bughole detection for concrete surface image based on deep learning, IEEE Access 9 (2021) 85709–85720, http://dx.doi.org/10.1109/access.2021.3088292.
[7] P.F.G. Banfill, M.A.O.M. Teixeira, R.J.M. Craik, Rheology and vibration of fresh concrete: Predicting the radius of action of poker vibrators from wave propagation, Cem. Concr. Res. 41 (9) (2011) 932–941, http://dx.doi.org/10.1016/j.cemconres.2011.04.011.
[8] Guillaume Grampeix, Nicolas Roussel, Jérôme Dupoirier, Internal vibration and viscous concrete: application and prediction of the radius of action, Rheol. Process. Constr. Mater. RILEM Proc. PRO 90 (2013) 123–130, https://www.afgc.asso.fr.
[9] Tao Cheng, Jochen Teizer, Giovanni C Migliaccio, Umberto C Gatti, Automated task-level activity analysis through fusion of real time location sensors and worker's thoracic posture data, Autom. Constr. 29 (2013) 24–39, http://dx.doi.org/10.1016/j.autcon.2012.08.003.
[10] Paul Teicholz, Labor-productivity declines in the construction industry: Causes and remedies (another look), AECbytes Viewpoint 67 (2013) 15, https://www.aecbytes.com/viewpoint/2013.
[11] Paul Teicholz, Paul M. Goodrum, Carl T. Haas, U.S. construction labor productivity trends, 1970–1998, J. Constr. Eng. Manage. 127 (5) (2001) 427–429, http://dx.doi.org/10.1061/(asce)0733-9364(2001)127:5(427).
[12] Wulong Gu, Mun S. Ho, A comparison of industrial productivity growth in Canada and the United States, Amer. Econ. Rev. 90 (2) (2000) 172–175, http://dx.doi.org/10.1257/aer.90.2.172.
[13] David Arditi, Krishna Mochtar, Trends in productivity improvement in the US construction industry, Constr. Manag. Econ. 18 (1) (2000) 15–27, http://dx.doi.org/10.1080/014461900370915.
[14] Soha Rawas, AI: the future of humanity, Discov. Artif. Intell. 4 (1) (2024) http://dx.doi.org/10.1007/s44163-024-00118-3.
[15] Beyza Topuz, Neşe Çakici Alp, Machine learning in architecture, Autom. Constr. 154 (2023) 105012, http://dx.doi.org/10.1016/j.autcon.2023.105012.
[16] Christian Janiesch, Patrick Zschech, Kai Heinrich, Machine learning and deep learning, Electron. Mark. 31 (3) (2021) 685–695, http://dx.doi.org/10.1007/s12525-021-00475-2.
[17] Yuhu Quan, Fenglai Wang, Machine learning-based real-time tracking for concrete vibration, Autom. Constr. 140 (2022) 104343, http://dx.doi.org/10.1016/j.autcon.2022.104343.
[18] Y.W. Chan, Yong-Guo Chen, Yi-Shi Liu, Effect of consolidation on bond of reinforcement in concrete of different workabilities, ACI Mater. J. 100 (2003) 294–301, http://dx.doi.org/10.14359/12667.
[19] Mikael P.J. Olsen, Energy requirements for consolidation of concrete during iinternal vibration, Spec. Publ. 96 (1987) 179–196, http://dx.doi.org/10.14359/3508.
[20] Michael F Petrou, Kent A Harries, Francis Gadala-Maria, Venkata Giri Kolli, A unique experimental method for monitoring aggregate settlement in concrete, Cem. Concr. Res. 30 (5) (2000) 809–816, http://dx.doi.org/10.1016/s0008-8846(00)00223-4.
[21] Zhenghong Tian, Ce Bian, Visual monitoring method on fresh concrete vibration, KSCE J. Civ. Eng. 18 (2) (2013) 398–408, http://dx.doi.org/10.1007/s12205-013-0475-x.
[22] Jie Gong, Yi Yu, Raghav Krishnamoorthy, Andrés Roda, Real-time tracking of concrete vibration effort for intelligent concrete consolidation, Autom. Constr. 54 (2015) 12–24, http://dx.doi.org/10.1016/j.autcon.2015.03.017.
[23] Zhenghong Tian, Xiao Sun, Weihao Su, Dongxin Li, Biao Yang, Ce Bian, Jun Wu, Development of real-time visual monitoring system for vibration effects on fresh concrete, Autom. Constr. 98 (2019) 61–71, http://dx.doi.org/10.1016/j.autcon.2018.11.025.
[24] Sang Gyu Lee, Miroslaw Jan Skibniewski, Monitoring of concrete placement and vibration for real-time quality control, in: Proceedings of the Creative Construction Conference 2019, Budapest University of Technology and Economics, 2019, http://dx.doi.org/10.3311/ccc2019-011.
[25] Sanggyu Lee, Miroslaw J. Skibniewski, Automated monitoring and warning solution for concrete placement and vibration workmanship quality issues, AI Civ. Eng. 1 (1) (2022) http://dx.doi.org/10.1007/s43503-022-00003-x.
[26] Jiajie Li, Zhenghong Tian, Xiao Sun, Yuanshan Ma, Hengrui Liu, Hao Lu, Modeling vibration energy transfer of fresh concrete and energy distribution visualization system, Constr. Build. Mater. 354 (2022) 129210, http://dx.doi.org/10.1016/j.conbuildmat.2022.129210.
[27] Jiajie Li, Zhenghong Tian, Xin Yu, Junzheng Xiang, Haoyue Fan, Vibration quality evaluation of reinforced concrete using energy transfer model, Constr. Build. Mater. 379 (2023) 131247, http://dx.doi.org/10.1016/j.conbuildmat.2023.131247.
[28] Denghua Zhong, Ziyang Shen, Jiajun Wang, Study on dynamic evaluation of vibration quality of concrete dam based on realtime monitoring(in Chinese), J. Hydraul. Eng. 49 (7) (2018) 775–786, https://link.oversea.cnki.net/doi/10.13243/j.cnki.slxb.20180122.
[29] Yajie Liu, Develop of Concrete Vibration Monitoring System based on Stereo Vision(In Chinese) (Dissertation for the Master Degree in Science), Harbin Institute of Technology, 2019, https://www.cnki.net.
[30] Botao Zhong, Haitao Wu, Lieyun Ding, Peter E.D. Love, Heng Li, Hanbin Luo, Li Jiao, Mapping computer vision research in construction: Developments, knowledge gaps and implications for research, Autom. Constr. 107 (2019) 102919, http://dx.doi.org/10.1016/j.autcon.2019.102919.
[31] Dong Wang, Bingyu Ren, Bo Cui, Jiajun Wang, Xiaoling Wang, Tao Guan, Real-time monitoring for vibration quality of fresh concrete using convolutional neural networks and IoT technology, Autom. Constr. 123 (2021) 103510, http://dx.doi.org/10.1016/j.autcon.2020.103510.
[32] Bingyu Ren, Haodong Wang, Dong Wang, Tao Guan, Xiaofeng Zheng, Vision method based on deep learning for detecting concrete vibration quality, Case Stud. Constr. Mater. 18 (2023) e02132, http://dx.doi.org/10.1016/j.cscm.2023.e02132.
[33] Fujia Wei, Gang Yao, Yang Yang, Yujia Sun, Instance-level recognition and quantification for concrete surface bughole based on deep learning, Autom. Constr. 107 (2019) 102920, http://dx.doi.org/10.1016/j.autcon.2019.102920.
[34] Jiajie Li, Zhenghong Tian, Xiao Sun, Yuanshan Ma, Hengrui Liu, Working state determination for concrete internal vibrator using genetic simulated annealing clustering method, Case Stud. Constr. Mater. 17 (2022) e01163, http://dx.doi.org/10.1016/j.cscm.2022.e01163.
[35] Hao Liu, Chengzhao Liu, Jiake Fu, Chenzhe Ma, Ye Zhang, Yumeng Lei, Intelligent analysis of hydraulic concrete vibration time based on convolutional neural network, in: Tayfun Dede (Ed.), Adv. Civ. Eng. 2023 (2023) 1–11, http://dx.doi.org/10.1155/2023/5530102.
[36] Yuanshan Ma, Zhenghong Tian, Xiaobin Xu, Hengrui Liu, Jiajie Li, Haoyue Fan, Research on response parameters and classification identification method of concrete vibration process, Materials 16 (8) (2023) 2958, http://dx.doi.org/10.3390/ma16082958.
[37] Stefan Nagel, Supervised learning, in: Machine Learning in Asset Pricing, Princeton University Press, 2021, pp. 11–30, http://dx.doi.org/10.23943/princeton/9780691218700.003.0002.
[38] Unsupervised learning, 2014, pp. 9–26, http://dx.doi.org/10.1002/9781118875568.ch2.
[39] Yayin Xu, Ying Zhou, Przemyslaw Sekula, Lieyun Ding, Machine learning in construction: From shallow to deep learning, Dev. Built Environ. 6 (2021) 100045, http://dx.doi.org/10.1016/j.dibe.2021.100045.

[40] Thomas P. Trappenberg, Reinforcement learning, in: Fundamentals of Machine Learning, Oxford University Press, 2019, pp. 206–232, http://dx.doi.org/10.1093/oso/9780198828044.003.0010.

[41] James Birnie, Alan Yates, Cost prediction using decision/risk analysis methodologies, Constr. Manag. Econ. 9 (2) (1991) 171–186, http://dx.doi.org/10.1080/01446199100000015.

[42] Brenda McCabe, Simaan M. AbouRizk, Randy Goebel, Belief networks for construction performance diagnostics, J. Comput. Civ. Eng. 12 (2) (1998) 93–100, http://dx.doi.org/10.1061/(asce)0887-3801(1998)12:2(93).

[43] Leonard E. Baum, Ted Petrie, Statistical inference for probabilistic functions of finite state Markov chains, Ann. Math. Stat. 37 (6) (1966) 1554–1563, http://dx.doi.org/10.1214/aoms/1177699147.

[44] Li Shu-quan, Zhao Xin-li, Lu Zhi-qiang, Fan Li-xia, Ma Lan, Gao Qiu-li, Dynamic monitoring on construction safety based on support vector machine, in: 2006 International Conference on Management Science and Engineering, IEEE, 2006, http://dx.doi.org/10.1109/icmse.2006.314150.

[45] Hyeonwoo Seong, Hyunchul Choi, Hyukman Cho, Sungwook Lee, Hyojoo Son, Changwan Kim, Vision-based safety vest detection in a construction scene, in: Proceedings of the 34th International Symposium on Automation and Robotics in Construction, ISARC, in: ISARC2017, Tribun EU, s.r.o., Brno, 2017, http://dx.doi.org/10.22260/isarc2017/0039.

[46] JuHyeong Ryu, JoonOh Seo, Houtan Jebelli, SangHyun Lee, Automated action recognition using an accelerometer-embedded wristband-type activity tracker, J. Constr. Eng. Manage. 145 (1) (2019) http://dx.doi.org/10.1061/(asce)co.1943-7862.0001579.

[47] Naser El-Sheimy, Haiying Hou, Xiaoji Niu, Analysis and modeling of inertial sensors using allan variance, IEEE Trans. Instrum. Meas. 57 (1) (2008) 140–149, http://dx.doi.org/10.1109/tim.2007.908635.

[48] Adam Coates, Andrew Y. Ng, Learning feature representations with K-means, in: Lecture Notes in Computer Science, Springer Berlin Heidelberg, 2012, pp. 561–580, http://dx.doi.org/10.1007/978-3-642-35289-8_30.

[49] Khaista Rehman, Paul W. Burton, Graeme A. Weatherill, K-means cluster analysis and seismicity partitioning for Pakistan, J. Seismol. 18 (3) (2013) 401–419, http://dx.doi.org/10.1007/s10950-013-9415-y.

[50] Trupti M. Kodinariya, Prashant R. Makwana, et al., Review on determining number of cluster in K-Means clustering, Int. J. 1 (6) (2013) 90–95, http://dx.doi.org/10.61161/ijarcsms.